Spurious multiples in seismic interferometry of primaries

Roel Snieder[1], Kees Wapenaar[2], and Ken Larner[1]
[1] *Center for Wave Phenomena, Colorado School of Mines, Golden CO 80401, email rsnieder@mines.edu,*
[2] *Dept. of Geotechnology, Delft University of Technology, Delft, The Netherlands*

ABSTRACT
Seismic interferometry yields the Green's function that accounts for wave propagation between receivers by correlating the waves recorded at these receivers. We present a derivation of this principle based on the method of stationary phase. Although this derivation is applicable to simple media only, it provides insight into the physical principle of seismic interferometry. In a homogeneous medium with one horizontal reflector and without a free surface, the correlation of the waves recorded at two receivers correctly gives both the direct wave and the single-reflected waves. When more reflectors are present a product of the single-reflected waves occurs in the cross correlation that leads to spurious multiples when the waves are excited at the surface only. We give a heuristic argument that these spurious multiples disappear when sources below the reflectors are included. We also extend the derivation to a smoothly varying inhomogeneous background medium.

Key words: siesmic interferometry, stationary phase, multiples

1 INTRODUCTION

Traditionally, imaging techniques are based on the illumination of an object by a coherent source. In many applications coherent sources are not available. Seismic interferometry is a technique in which the Green's function that describes the waves that propagate between two receivers is extracted by computing the correlation of signals recorded at these two receivers. These signals may have been excited by either coherent or incoherent sources. The advantages of this technique are that incoherent noise can be the source of the waves used for imaging and that one can effectively use a wavefield that is excited at one of the receivers, even though no physical source exists at that location.

The first formulation of this technique is due to Claerbout [1968] , who used the phrase "daylight imaging" because the daylight that we use in our vision also provides an incoherent illumination of the objects that we view. His derivation was applicable to layered media. The emergence of the Green's function was subsequently derived for general media using normal-mode theory [Lobkis and Weaver, 2001]. That derivation is applicable only for finite media that have a discrete frequency spectrum. This requirement was relaxed in an alternative derivation based on the representation theorem for one-way wave propagation [Wapenaar et al., 2004], and by using the general representation theorem [Weaver and Lobkis, 2004; Wapenaar, 2004]. Alternative, but equivalent proofs of the emergence of the Green's function have been formulated using the principle of time-reversed imaging [Derode et al., 2003ab; Bakulin and Calvert, 2004; Roux and Fink, 2003]. The relationship between these approaches is shown by Wapenaar et al. [2004] .

The reconstruction of the Green's function from recordings of incoherent signals has been shown observationally using ultrasound [Weaver and Lbkis, 2001; Larose et al., 2004; Malcolm et al., 2004]. Seismic interferometry has been used in helioseismology [Rickett and Claerbout, 1999; Rickett and Claerbout, 2000], in exploration seismology [Bakulin and Calvert, 2004; Schuster et al., 2004], in crustal seismology for the retrieval of the surface wave Green's function [Campillo and Paul, 2003; Shapiro and Campillo, 2004; Shapiro et al., 2005],

and for extracting the response of buildings from an incoherent excitation [Snieder, 2005].

The mechanism of seismic interferometry can be explained using the method of stationary phase [Snieder, 2004a]. This is not surprising because the stationary phase approximation is the natural tool to account for the destructive and constructive interference that forms the physical basis of seismic interferometry. The derivation of seismic interferometry with the principle of stationary phase is approximate, but, as shown by Roux et al. [2005] , the stationary phase integral can also be evaluated exactly using elliptical coordinates. This gives exactly the same final result as the stationary phase approximation. The derivation of seismic interferometry based on stationary phase has also been used for waves in a waveguide [Sabra et al., 2005].

The derivation of stationary phase is applicable for simple media only where one can easily account for the different rays that propagate through the media. In this sense the derivation based on stationary phase is less general than derivations based on normal modes, representation theorems, or time-reversed imaging. Despite this limitation, the derivation based on stationary phase is useful because it sheds light on the physics that underlies seismic interferometry. The value of this derivation is mostly didactic, but it also highlights sampling issues and the generation of spurious multiples.

Here we show that singly reflected waves that propagate between two receivers in the subsurface can correctly be reproduced by correlating the waves that have been excited by uncorrelated sources at the surface and are recorded at the two receivers. We derive this for the simplest case for a homogeneous medium without a free surface and flat horizontal reflectors in the subsurface.

In section 2, we derive the general framework for illumination of the subsurface by incoherent sources, and introduce the employed single-scattering model in section 3. In section 4 we show how this leads to the retrieval of the direct wave that propagates between the receivers, and, in section 5, we show that this procedure also correctly leads to the single-reflected wave that propagates between the receivers. The correlation of the single-reflected waves leads to a contribution that is proportional to the square of the reflection coefficient. We show in section 6 that this term is kinematically equivalent to the direct wave that propagates between the receivers. In section 7 we show a numerical example that illustrates the role of stationary phase in seismic interferometry. In section 8, we generalize the derivation to the case of a layered medium with more than one reflector, and we show that the product of singly-reflected waves from different reflectors gives a nonzero contribution to the cross-correlation. We refer to these terms as *spurious multiples* because these terms depend on the product of reflection coefficients, just like real multiples do. The spurious multiples, however, have arrival times that differ from those of real multiples.

2 ILLUMINATING THE SUBSURFACE FROM SOURCES AT THE SURFACE

Consider the problem wherein many sources at the surface $z = 0$ illuminate the subsurface. These sources can be either coherent or incoherent, and the may act either simultaneously or sequentially. The sources are placed at locations $\mathbf{r}_S = (x, y, 0)$ and have a source-time signal $S_S(t)$ that corresponds in the frequency domain to the complex spectrum $S_S(\omega)$. The Earth response that is excited by these sources is recorded at two receivers at locations $\mathbf{r}_A = (x_A, 0, z_A)$ and $\mathbf{r}_B = (x_B, 0, z_B)$, respectively. Without loss of generality, we align the x-axis of the employed coordinate system with the horizontal separation of the sources; hence in this coordinate system the y-coordinate of both sources vanishes.

The source-time functions $S_S(t)$ may be impulsive, but they might also correspond to functions with a more random character, as would be excited by, for example, traffic noise in a land survey or wave noise at the sea-surface during a marine survey. In the sequel we assume that the source time functions for sources at $\mathbf{r}_S$ and $\mathbf{r}_{S'}$ are uncorrelated when averaged over time and that the power spectrum of the source time functions is identical:

$$\int_0^{T_{aver}} S_S(t) S_{S'}(t+\tau) dt = \delta_{SS'} C(\tau) \ , \qquad (1)$$

where T_{aver} denotes the length of the time-averaging and $C(\tau)$ the autocorrelation of the source time functions. The autocorrelation is the Fourier transform of the power spectrum. Since all sources are assumed to have the same power spectrum, they have the same autocorrelation as well.

The source-time functions may have a different character in different imaging experiments. In the virtual-source experiments of Bakulin and Calvert [2004] the shots do not overlap in time. The shots are recorded and processed one after the other, and the cross terms between the shots in expression (1) by definition vanish. The situation is more complicated when truly incoherent sources illuminate the surface. Consider for example the seismic noise generated by waves at the sea-surface. The seismic waves excited at different locations on average are uncorrelated. Snieder [Snieder, 2004a] has shown that for random sources the ensemble average of expression (1) vanishes and that, in a single realization, the ratio of the cross term $S \neq S'$ to the diagonal term $S = S'$ is given by

$$\frac{|\text{cross terms}|}{|\text{diagonal terms}|} \sim \sqrt{\frac{t_{corr}}{N_{sources} T_{aver}}} \ , \qquad (2)$$

where $N_{sources}$ denotes the number of sources and t_{corr} is the temporal width of the cross-correlation $C(\tau)$. This width is inversely proportional to the bandwidth Δf of the sources. The product of the bandwidth and the averaging length T_{aver} is equal to $N_{freedom}$, the number of degrees of freedom in the data [Landau, 1967; Bucci and Franceschetti, 1989]. Therefore the ratio of the cross

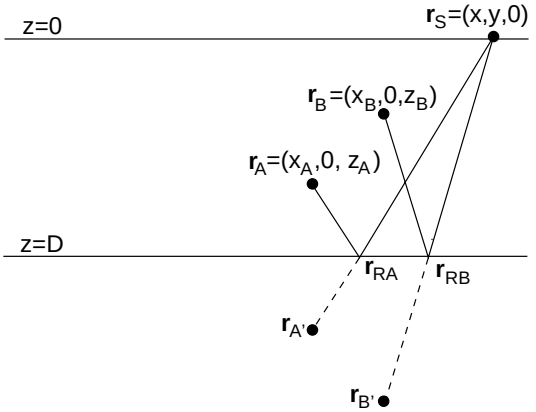

Figure 1. The geometry of an imaging experiment with a source at the surface and two receivers at $\mathbf{r}_A$ and $\mathbf{r}_B$. The mirror image of these receivers in the reflector is indicated at the locations $\mathbf{r}_{A'}$ and $\mathbf{r}_{B'}$, respectively.

terms to the diagonal terms in a single realization is equal to

$$\frac{|\text{cross terms}|}{|\text{diagonal terms}|} \sim \frac{1}{\sqrt{N_{sources} N_{freedom}}} \ . \qquad (3)$$

It follows from expression (2) that for random, incoherent, source-time functions the cross terms can be made arbitrarily small by increasing the length of the time window over which the averaging is carried out. In the following we assume that the cross-terms $S \neq S'$ can be ignored altogether. In that case, expression (1) corresponds in the frequency domain to

$$S_S(\omega) S_{S'}(\omega) = \delta_{SS'} \left|S(\omega)\right|^2 \ . \qquad (4)$$

This condition of uncorrelated sources was also used by Wapenaar [2004] , who assumed that the sources are located in the deep subsurface.

We now consider correlation of the waves recorded at two receivers for the special case of an acoustic medium. The waves recorded at the receivers A and B are given by

$$\begin{aligned} u_A(\omega) &= \textstyle\sum_S G^{full}(\mathbf{r}_A, \mathbf{r}_S, \omega) S_S(\omega) \ , \\ u_B(\omega) &= \textstyle\sum_S G^{full}(\mathbf{r}_B, \mathbf{r}_S, \omega) S_S(\omega) \ , \end{aligned} \qquad (5)$$

with G^{full} the full Green's function which consists of the direct wave, primaries, and multiples. In the frequency domain the temporal correlation of the waves recorded is given by

$$C_{AB}(\omega) = u_A(\omega) u_B^*(\omega) \ , \qquad (6)$$

where the asterisk denotes the complex conjugate. Inserting equation (5) in the previous expression gives

$$C_{AB}(\omega) = \sum_{S,S'} G^{full}(\mathbf{r}_A, \mathbf{r}_S) G^{full*}(\mathbf{r}_B, \mathbf{r}_{S'}) S_S(\omega) S_{S'}^*(\omega) \ . \qquad (7)$$

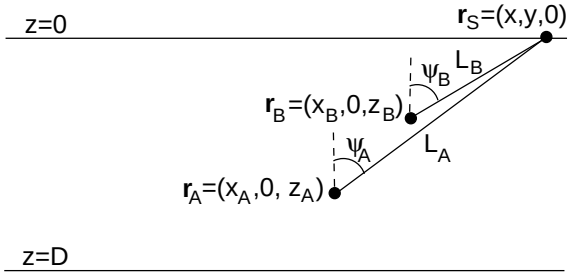

Figure 2. Definition of the geometric variables in the analysis of term 1.

Since the sources are uncorrelated, as stated in expression (4), the cross-terms $S \neq S'$ in this double sum vanish; hence

$$C_{AB}(\omega) = \sum_S G^{full}(\mathbf{r}_A, \mathbf{r}_S) G^{full*}(\mathbf{r}_B, \mathbf{r}_S) \left|S(\omega)\right|^2 \ . \qquad (8)$$

When the sources are densely distributed along the surface, with n sources per unit surface area, the sum over sources can be replaced by an integration: $\sum_S(\cdots) \rightarrow n \int(\cdots) dx$ over the surface; this gives

$$C_{AB}(\omega) = \left|S(\omega)\right|^2 n \int G^{full}(\mathbf{r}_A, \mathbf{r}_S) G^{full*}(\mathbf{r}_B, \mathbf{r}_S) dx dy \ , \qquad (9)$$

with x and y the coordinates of the source at the surface as shown in figure 1.

3 A SINGLE-SCATTERING MODEL

In order to better understand the physics of seismic interferometry, we illustrate this technique with a model that consists of a single reflector with plane-wave reflection coefficient r that is embedded in a homogeneous medium. The Green's function in the homogeneous medium is given by

$$G(R) = -\frac{e^{ikR}}{4\pi R} \ , \qquad (10)$$

with the wavenumber given by $k = \omega/c$, c the wave velocity, and R the distance of propagation. We presume that there is no free surface, so this model does not include any multiply reflected waves. As shown in figure 1, $\mathbf{r}_{RA}$ denotes the reflection point of the wave that propagates to $\mathbf{r}_A$. The full Green's function is the superposition of the direct wave and the single-reflected wave:

$$\begin{aligned} G^{full}(\mathbf{r}_A, \mathbf{r}_S) &= G(|\mathbf{r}_A - \mathbf{r}_S|) \\ &\quad + r\, G(|\mathbf{r}_A - \mathbf{r}_{RA}| + |\mathbf{r}_{RA} - \mathbf{r}_S|) \ , \\ G^{full}(\mathbf{r}_B, \mathbf{r}_S) &= G(|\mathbf{r}_B - \mathbf{r}_S|) \\ &\quad + r\, G(|\mathbf{r}_B - \mathbf{r}_{RB}| + |\mathbf{r}_{RB} - \mathbf{r}_S|) \ . \end{aligned} \qquad (11)$$

In this expression, we used that the reflected wave is given by the Green's function that accounts for the propagation from the source to an image point of the receiver below the reflector. The image points of the receivers A and B are indicated in figure 1 by $\mathbf{r}'_A$ and $\mathbf{r}'_B$, respectively. As shown in that figure, for receiver A the total distance covered by the reflected wave is $|\mathbf{r}_A - \mathbf{r}_{RA}| + |\mathbf{r}_{RA} - \mathbf{r}_S|$.

Inserting equation (11) into expression (9) gives an expression for the correlation, which consists of a sum of four terms:

$$\begin{aligned} C_{AB}(\omega) \quad &= n\,|S(\omega)|^2 \underbrace{\int G(|\mathbf{r}_A - \mathbf{r}|)G^*(|\mathbf{r}_B - \mathbf{r}|)dxdy}_{T1} \\ &+n\,|S(\omega)|^2\, r \underbrace{\int G(|\mathbf{r}_A - \mathbf{r}|)G^*(|\mathbf{r}_B - \mathbf{r}_{RB}| + |\mathbf{r}_{RB} - \mathbf{r}|)dxdy}_{T2} \\ &+n\,|S(\omega)|^2\, r \underbrace{\int G(|\mathbf{r}_A - \mathbf{r}_{RA}| + |\mathbf{r}_{RA} - \mathbf{r}|)G^*(|\mathbf{r}_B - \mathbf{r}|)dxdy}_{T3} \\ &+n\,|S(\omega)|^2\, r^2 \underbrace{\int G(|\mathbf{r}_A - \mathbf{r}_{RA}| + |\mathbf{r}_{RA} - \mathbf{r}|)G^*(|\mathbf{r}_B - \mathbf{r}_{RB}| + |\mathbf{r}_{RB} - \mathbf{r}|)dxdy}_{T4} . \end{aligned} \tag{12}$$

Term 1 (T1) is the correlation of the direct waves that propagate to the two receivers; this term does not depend on the reflection coefficient. Terms 2 and 3 are proportional to the reflection coefficient r, for this reason they can be expected to account for the single-reflected waves in the Green's function that are extracted from the correlation. Term 4 depends on r^2. In the following, we analyze terms 1-4 in order to establish the connection between the correlation and the Green's function for this simple wave propagation problem.

4 ANALYSIS OF TERM 1

The derivation shown in this section is similar to that in an earlier analysis [Snieder, 2004a]. Using the lengths L_A and L_B, as defined in figure 2, and the Green's function (10), term 1 can be written as

$$T1 = \frac{1}{(4\pi)^2} \int \frac{\exp\left(ik\left(L_A - L_B\right)\right)}{L_A L_B} dxdy\ . \tag{13}$$

The integrand has an oscillatory character, but as we will see, the integrand has a stationary point. For this reason we analyze this integral in the stationary phase approximation [Bleistein, 1984; Snieder, 2004b]. Referring to figure 2, the lengths $L_{A,B}$ are given by

$$L_{A,B} = \sqrt{\left(x - x_{A,B}\right)^2 + y^2 + z_{A,B}^2}\ . \tag{14}$$

The stationary point of the integrand follows by setting the partial x- and y-derivatives of $L = L_A - L_B$ equal to zero. For the y-derivative this gives

$$0 = \frac{\partial L}{\partial y} = \frac{y}{L_A} - \frac{y}{L_B}\ . \tag{15}$$

This derivative vanishes for $y = 0$; hence the condition of stationarity with respect to y implies that the stationary source point lies in the vertical plane of the receivers. The stationarity condition with respect to the x-coordinate gives

$$0 = \frac{\partial L}{\partial x} = \frac{x - x_A}{L_A} - \frac{x - x_B}{L_B} = \sin\psi_A - \sin\psi_B\ , \tag{16}$$

where the angles ψ_A and ψ_B are defined in figure 2. The phase thus is stationary when

$$\psi_A = \psi_B \qquad \text{and} \qquad y = 0\ . \tag{17}$$

The stationarity condition $\psi_A = \psi_B$ is illustrated in figure 3; it implies that the stationary source point at the surface is aligned with the line joining the two receivers. In these figures the receivers are at different depths.

Note that when the receivers are at the same depth ($z_A = z_B$) there is no stationary source position, except for sources infinitely far away. Any attenuation will suppress the contribution of those sources.

Kinematically, expression (13) gives a contribution at a lag-time that is equal to the time it takes for the wave to propagate from receiver B to receiver A because the wave that propagates along the path shown in figure 3 arrives at receiver A with a time delay $|\mathbf{r}_A - \mathbf{r}_B|/c$ compared to the wave that arrives at receiver B. It is nontrivial that the evaluation of the integral in (13) gives a contribution that is also dynamically equal to the Green's function of the waves that propagate between the receivers A and B. In the following we evaluate the integral in the stationary phase approximation.

Evaluating the second derivatives of $L = L_A - L_B$ while using (17) for the stationary point gives

$$\begin{aligned} \frac{\partial^2 L}{\partial x^2} &= \frac{z_A^2}{L_A^3} - \frac{z_B^2}{L_B^3} = \frac{z_A^2}{L_A^2}\frac{1}{L_A} - \frac{z_B^2}{L_B^2}\frac{1}{L_B} \\ &= \cos^2\psi \left(\frac{1}{L_A} - \frac{1}{L_B}\right) , \end{aligned} \tag{18}$$

and

$$\frac{\partial^2 L}{\partial y^2} = \frac{L_A^2}{L_A^3} - \frac{L_B^2}{L_B^3} = \frac{1}{L_A} - \frac{1}{L_B} . \tag{19}$$

In this example, and the following examples, $\partial^2 L/\partial x \partial y = 0$ at the stationary point, and the two-dimensional stationary phase integral reduces to the product of two one-dimensional stationary phase integrals over the x- and y-coordinates, respectively.

In the following, L_A and L_B are the path lengths for the stationary source position as shown in figure 3. Note that in the geometry of figure 3, $L_A > L_B$ so that $L_A^{-1} - L_B^{-1} < 0$. Evaluating the integral (13) in the stationary phase approximation thus gives

$$\begin{aligned} T1 &= \frac{1}{(4\pi)^2}\frac{\exp\left(ik\left(L_A - L_B\right)\right)}{L_A L_B} \\ &\times e^{-i\pi/4}\sqrt{\frac{2\pi}{k}}\frac{1}{\sqrt{\cos^2\psi\left(\frac{1}{L_B} - \frac{1}{L_A}\right)}} \\ &\times e^{-i\pi/4}\sqrt{\frac{2\pi}{k}}\frac{1}{\sqrt{\frac{1}{L_B} - \frac{1}{L_A}}} , \end{aligned} \tag{20}$$

Using the relation $k = \omega/c$, we can write this expression as

$$T1 = \frac{c}{8\pi(-i\omega)\cos\psi}\frac{\exp\left(ik\left(L_A - L_B\right)\right)}{L_A - L_B} , \tag{21}$$

The distance $L_A - L_B$ is equal to the receiver separation R shown in figure 3. With expression (10) and including the factor $n\,|S(\omega)|^2$ of expression (12), this gives a total contribution that is equal to

$$T1 = \frac{n\,|S(\omega)|^2\,c}{2\cos\psi} \times \frac{G(R)}{-i\omega} . \tag{22}$$

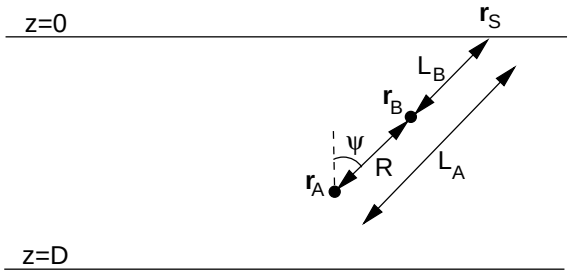

Figure 3. Definition of the geometric variables for the stationary source position in term 1.

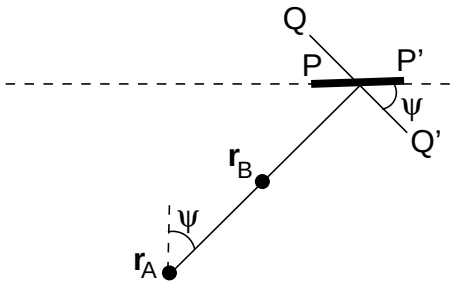

Figure 4. The relation between an element PP' along the surface and the corresponding element QQ' perpendicular to the receiver line.

This means that the contribution of term 1 to the correlation is, in the frequency domain, proportional to the Green's function of the direct wave that propagates between the receivers. Note that this Green's function is multiplied by the source density n at the surface; a denser source distribution gives a stronger correlation than does a less dense one. The Green's function is also multiplied by the power spectrum $|S(\omega)|^2$ of the sources. This power spectrum can be measured, and one can correct for this term. In order to retrieve the Green's function from term 1, one needs to multiply with $-i\omega$. Because of the employed Fourier transform, $f(t) = \int F(\omega)\exp(-i\omega t)d\omega$, this multiplication corresponds to a differentiation in the time domain. This differentiation corrects for the integration that is carried out in the cross-correlation. This need to carry out the differentiation was also noted in other formulations of seismic interferometry, e.g., [Lobkis and Weaver, 2001; Snieder, 2004a; Weaver and Lobkis, 2004].

The term $\cos\psi$ in the denominator is an obliquity factor that corrects for the fact that the length element QQ' of figure 4 perpendicular to the ray corresponds to a line element PP' along the surface whose lengths that are related by $QQ' = PP'/\cos\psi$.

In the virtual-source experiment of Bakulin and

Calvert [2004], the sources at the surface were placed in a line. In that case there is no integration over the y-coordinate, and the latter terms in expression (20) that come from the y-integration are absent; in that case

$$T1_{line} = \frac{in\,|S(\omega)|^2\,\sqrt{c}}{\sqrt{8\pi}\sqrt{-i\omega}\cos\psi}\sqrt{\frac{1}{L_B}-\frac{1}{L_A}}\;G(R)\;. \quad (23)$$

Note the presence of the factor i and the term $1/\sqrt{-i\omega}$. Correcting for these terms involves a Hilbert transform and a fractional derivative. These correction factors are common in two-dimensional imaging experiments [Yilmaz, 1987; Bleistein et al., 2001; Haney and Snieder, 2005]. Without these corrections the reconstructed Green's function does not have the proper phase and frequency dependence. More seriously, in contrast to equation (22), expression (23) depends explicitly on the distances L_A and L_B. It turns out that when the derivation leading to expression (23) is repeated using the Green's function in two dimensions, an expression analogous to equation (22) is obtained. The presence of the fractional derivatives and the lengths L_A and L_B is thus due to a mismatch between the dimensionality of the physical space through which the waves propagate (3D versus 2D) and the dimensionality of the source distribution (2D versus 1D). The derivation of seismic interferometry by Roux and Fink [2003] is based on wave propagation in three dimensions, while the employed sources are placed along a line. As shown by the example of expression (23), this leads to a Green's function that is kinematically correct, but whose amplitude and phase is not.

A complex overburden located between the surface sources and the receivers in the subsurface acts as a diffusor of seismic waves because the waves radiated from a single source arrive at a receiver from various directions resulting from the scattering and multipathing that has occurred in the overburden. In the experiment of Bukulin and Calvert [2004] the shots were placed on a line at the surface, but the complex overburden in their experiment created multipathing that provided a more diffuse illumination of their receivers in the subsurface that helps to focus the waves onto the virtual sources.

The analysis of this section can be generalized for a heterogeneous medium in which the velocity is sufficiently smooth to warrant the use of ray theory. We show in appendix A that term 1 is then given by

$$T1 = \sum_{stat.\ points} \frac{n|S(\omega)|^2 v_S}{2\cos\psi} \times \frac{G^{ray}(\mathbf{r}_A,\mathbf{r}_B)}{-i\omega}\;, \quad (24)$$

where $G^{ray}(\mathbf{r}_A,\mathbf{r}_B)$ is the ray-geometric Green's function for the waves recorded at $\mathbf{r}_A$ that are generated by a point source at $\mathbf{r}_B$. The summation in this expression is over all the stationary source points on the surface $z=0$. These points can be found by tracing rays from $\mathbf{r}_A$ to $\mathbf{r}_B$ and by extending these rays to the surface $z=0$. The angle ψ is the angle between these rays at the surface and the vertical, while v_S is the velocity at the intersection of these rays with the surface.

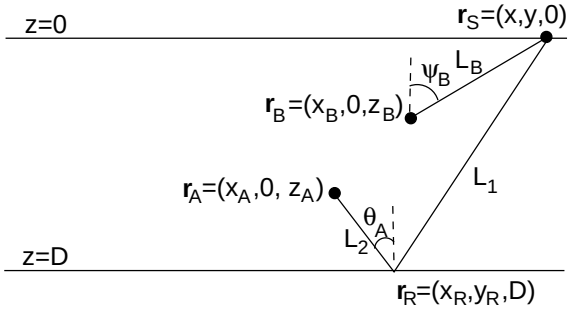

Figure 5. Definition of the geometric variables in the analysis of term 3.

5 ANALYSIS OF TERM 3

The analysis of this term could be achieved by applying the theory of the previous sections to receivers at the image points $\mathbf{r}_{A'}$ and $\mathbf{r}_{B'}$ of figure 1. Here we show explicitly that the cross-correlation correctly produces the single-reflected waves. Using the lengths defined in figure 5 this term is given by

$$T3 = \frac{1}{(4\pi)^2}\int \frac{\exp\left(ik\left(L_1+L_2-L_B\right)\right)}{\left(L_1+L_2\right)L_B}dxdy\;. \quad (25)$$

Before we can analyze this expression we need the coordinates of the reflection point $\mathbf{r}_R$ because this determines the lengths L_1 and L_2. The condition that the reflection angle is equal to angle of incidence gives

$$\begin{aligned} x_R &= \frac{\left(D-z_A\right)x + Dx_A}{2D-z_A}\;, \\ y_R &= \frac{\left(D-z_A\right)y}{2D-z_A}\;. \end{aligned} \quad (26)$$

Using this, the lengths $L_1$and L_2 are given by

$$\begin{aligned} L_1^2 = &\left(\frac{D}{2D-z_A}\right)^2(x-x_A)^2 \\ &+\left(\frac{D}{2D-z_A}\right)^2 y^2 + D^2\;, \end{aligned} \quad (27)$$

and

$$\begin{aligned} L_2^2 = &\left(\frac{D-z_A}{2D-z_A}\right)^2(x-x_A)^2 \\ &+\left(\frac{D-z_A}{2D-z_A}\right)^2 y^2 + (D-z_A)^2\;, \end{aligned} \quad (28)$$

while L_B is given by expression (14).

The stationary points of the integral (25) follow

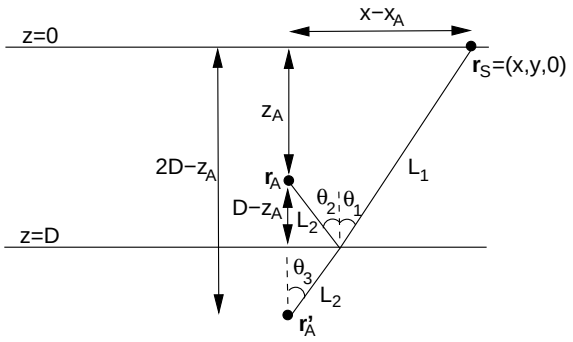

Figure 6. The angles θ_1, θ_2, and θ_3 and their relation to the geometric variables for the reflected wave.

from the first partial derivatives of $L = L_1 + L_2 - L_B$:

$$0 = \frac{\partial L}{\partial y} = \left(\frac{D}{2D - z_A}\right)^2 \left(\frac{y}{L_1}\right) + \left(\frac{D - z_A}{2D - z_A}\right)^2 \left(\frac{y}{L_2}\right) - \frac{y}{L_B} . \tag{29}$$

Again, the stationary source position occurs for $y = 0$; it is located in the vertical plane of the receivers. The condition for stationarity in the x-direction is

$$0 = \frac{\partial L}{\partial x} = \left(\frac{D}{2D - z_A}\right)^2 \left(\frac{x - x_A}{L_1}\right) + \left(\frac{D - z_A}{2D - z_A}\right)^2 \left(\frac{x - x_A}{L_2}\right) - \frac{x - x_B}{L_B} . \tag{30}$$

In order to interpret this last condition geometrically it is useful to relate the ratios in this expression to the angle of incidence at the reflector. Referring to figure 6, the following identities hold: $\cos\theta_1 = D/L_1$, $\cos\theta_2 = (D - z_A)/L_2$, and $\cos\theta_3 = (2D - z_A)/(L_1 + L_2)$. Since these angles are all equal to the angle of incidence θ_A of the reflected wave, we obtain:

$$\cos\theta_A = \frac{D}{L_1} = \frac{D - z_A}{L_2} = \frac{2D - z_A}{L_1 + L_2} . \tag{31}$$

Also, since $x - x_A = L_1 \sin\theta_1 + L_2 \sin\theta_2$, and since both angles are equal to θ_A,

$$\sin\theta_A = \frac{x - x_A}{L_1 + L_2} . \tag{32}$$

Dividing this expression by the last identity of (31) gives

$$\tan\theta_A = \frac{x - x_A}{2D - z_A} . \tag{33}$$

Finally, from (31),

$$\frac{D}{2D - z_A} = \frac{L_1}{L_1 + L_2} , \quad \frac{D - z_A}{2D - z_A} = \frac{L_2}{L_1 + L_2} . \tag{34}$$

Using expression (34) in (30), and using (32) to eliminate $x - x_A$, gives, with the relation $(x - x_B)/L_B = \sin\psi_B$,

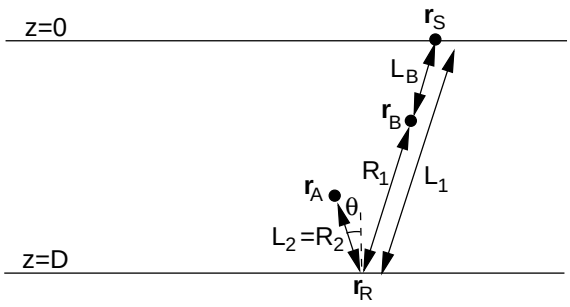

Figure 7. Definition of the geometric variables for the stationary source position for the analysis of term 3.

$$0 = \frac{\partial L}{\partial x} = \sin\theta_A - \sin\psi_B . \tag{35}$$

The integrand thus is stationary when the source position satisfies

$$\theta_A = \psi_B \qquad \text{and} \qquad y = 0 . \tag{36}$$

This condition is depicted in figure 7: waves radiated from the stationary source position at the surface travel in a straight line from the source through receiver B via a specular reflection to receiver A. Just as in the analysis of term 1, the time delay of this wave recorded at the two receivers is equal to the time it takes the wave to travel from receiver B via the reflector to receiver A. Thus the correlation is kinematically equal to the Green's function for the reflected waves. With the following stationary phase evaluation of the integral (25), we verify that the retrieved Green's function is also dynamically correct.

From expression (27) we get at the stationary point

$$\frac{\partial^2 L_1}{\partial x^2} = \left(\frac{D}{2D - z_A}\right)^2 \frac{D^2}{L_1^3} = \left(\frac{L_1}{L_1 + L_2}\right)^2 \frac{D^2}{L_1^2} \frac{1}{L_1} = \frac{L_1}{(L_1 + L_2)^2} \cos^2\theta . \tag{37}$$

In the second identity we have used expression (34), while the last identity follows from equation (31). In a similar way it follows that

$$\frac{\partial^2 L_2}{\partial x^2} = \frac{L_2}{(L_1 + L_2)^2} \cos^2\theta , \tag{38}$$

and, using (18), we obtain for the curvature of L_B,

$$\frac{\partial^2 L_B}{\partial x^2} = \frac{1}{L_B} \cos^2\theta . \tag{39}$$

In the last expression, we used the stationary phase condition $\psi = \theta$. Combining these results in the path difference $L = L_1 + L_2 - L_B$ gives

$$\frac{\partial^2 L}{\partial x^2} = \cos^2\theta \left(\frac{1}{L_1 + L_2} - \frac{1}{L_B}\right) . \tag{40}$$

Differentiation of (27) gives

$$\frac{\partial^2 L_1}{\partial y^2} \quad \left\{ \left(\frac{D}{2D - z_A} \right)^4 (x - x_A)^2 + \left(\frac{D}{2D - z_A} \right)^2 D^2 \right\} / L_1^3 \, . \tag{41}$$

With expressions (33) and (34) this is equal to

$$\frac{\partial^2 L_1}{\partial y^2} = \left(\frac{D}{L_1} \right)^2 \frac{1}{L_1} \left(\frac{L_1}{L_1 + L_2} \right)^2 \left(\tan^2 \theta + 1 \right) \, . \tag{42}$$

Using the identity $D/L_1 = \cos\theta$ this gives

$$\frac{\partial^2 L_1}{\partial y^2} = \frac{L_1}{(L_1 + L_2)^2} \, . \tag{43}$$

A similar analysis for L_2 gives

$$\frac{\partial^2 L_2}{\partial y^2} = \frac{L_2}{(L_1 + L_2)^2} \, . \tag{44}$$

This gives, for the curvature of L with respect to y,

$$\frac{\partial^2 L}{\partial y^2} = \frac{1}{L_1 + L_2} - \frac{1}{L_B} \, . \tag{45}$$

In these expressions it is understood that all lengths are evaluated at the stationary point.

The stationary phase evaluation of the integral (25) can now be carried out. Keeping in mind that $(L_1 + L_2)^{-1} - L_B^{-1} < 0$, and using the same steps as in section 4, gives

$$T3 = \frac{1}{(4\pi)^2} \frac{\exp(ik(L_1 + L_2 - L_B))}{(L_1 + L_2) L_B} \left(e^{-i\pi/4} \right)^2 \times \frac{2\pi}{k \cos\theta} \left(\frac{1}{L_B} - \frac{1}{L_1 + L_2} \right)^{-1} \, . \tag{46}$$

As shown in figure 7, $L_1 - L_B = R_1$, and $L_2 = R_2$. With the definition (10) for the Green's function this gives after taking the $rn\,|S(\omega)|^2$ terms into account:

$$T3 = \frac{n\,|S(\omega)|^2\, c}{2\cos\psi} \times r \frac{G(R_1 + R_2)}{-i\omega} \, . \tag{47}$$

Note the resemblance with expression (22) for the contribution of term 1 that gives the direct wave that propagates between the receiver. Expression (47) shows that the contribution of term 3 leads to the singly-reflected wave that propagates from receiver B via the reflector to receiver A. The same corrections must be applied to this term as to term 1 as discussed in section 4.

The same analysis can be applied to term 2 of expression (12), the final result is the complex conjugate of expression (47) so that

$$T2 = \frac{n\,|S(\omega)|^2\, c}{2\cos\psi} \times r \left(\frac{G(R_1 + R_2)}{-i\omega} \right)^* \, . \tag{48}$$

The stationary point now lies at the location on the surface such that the direct wave from the source to receiver A propagates along the same path as the wave that travels from the source to the reflector, and ultimately to receiver B.

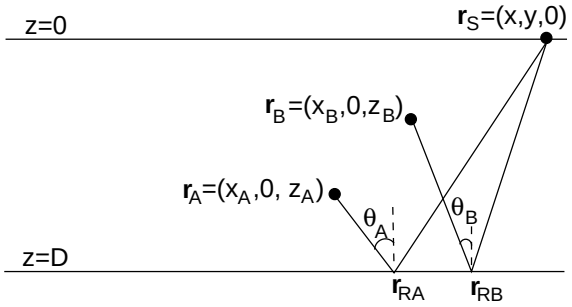

Figure 8. Definition of the geometric variables in the analysis of term 4.

The Green's function in expression (47) is the causal Green's function, while its complex conjugate in equation (48) is the acausal Green's function. It is known that seismic interferometry gives the superposition of the causal and the acausal Green's function [Lobkis and Weaver, 2001; Derode et al., 2003a; Malcolm et al., 2004; Derode et al., 2003b]. The causal Green's function can easily be retrieved from the cross-correlation either by truncating the cross-correlation for $t < 0$, or by averaging the cross-correlation for negative times and positive times.

6 ANALYSIS OF TERM 4

For the analysis of term 4, we carry out the stationary phase analysis of the following integral:

$$T4 = \frac{1}{(4\pi)^2} \int \frac{\exp(ikL)}{X} dx dy \, , \tag{49}$$

with

$$L = |\mathbf{r}_A - \mathbf{r}_{RA}| + |\mathbf{r}_{RA} - \mathbf{r}_S| - |\mathbf{r}_B - \mathbf{r}_{RB}| - |\mathbf{r}_{RB} - \mathbf{r}_S| \tag{50}$$

and

$$X = (|\mathbf{r}_A - \mathbf{r}_{RA}| + |\mathbf{r}_{RA} - \mathbf{r}_S|) \times (|\mathbf{r}_B - \mathbf{r}_{RB}| + |\mathbf{r}_{RB} - \mathbf{r}_S|) \tag{51}$$

where all variables are defined in figure 8. The stationary point follows from setting the x- and y-derivatives of the phase equal to zero. As in the previous sections, the stationarity condition with respect to y leads to the condition $y = 0$; this means again that the stationary point lies in the vertical plane of the receivers. Using the same steps that led to expression (35), one finds that the stationarity condition with respect to x is given by

$$0 = \frac{\partial L}{\partial x} = \sin\theta_A - \sin\theta_B \, , \tag{52}$$

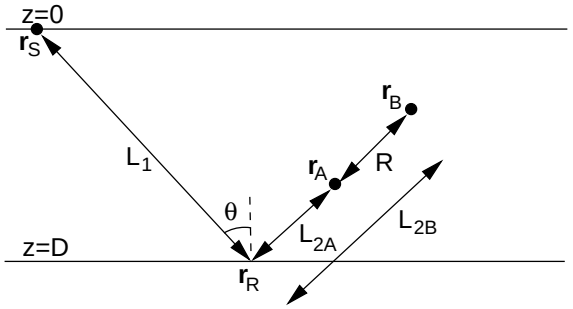

Figure 9. Definition of the geometric variables in the analysis of term 4 for the stationary source position.

where the angles θ_A and θ_B are defined in figure 8. The point of stationary phase thus is defined by the conditions

$$\theta_A = \theta_B \qquad \text{and} \qquad y = 0\ . \tag{53}$$

This condition of stationary phase corresponds to the source position shown in figure 9. The stationary source position launches two waves that, after reflection at the interface, both propagate along the line that joins the receivers. Since both reflected waves are proportional to r, this contribution to the correlation is proportional to r^2. The correlation of the waves shown in figure 9 is nonzero for a lag-time that is equal to the time it takes for the waves to propagate between the receivers. Kinematically, this term can thus be expected to correspond to the Green's function of the direct wave that propagates between the receivers.

In order to carry out the stationary phase analysis, the second derivatives of the phase is needed. These derivatives follow from the expressions (37), (38), (43) and (44). Using the lengths defined in figure 9, term 4 is given in the stationary phase approximation by

$$T4 \quad = \frac{1}{(4\pi)^2} \frac{\exp(ik(L_1 + L_{2A} - L_1 - L_{2B}))}{(L_1 + L_{2A})(L_1 + L_{2B})} \left(e^{-i\pi/4}\right)^2 \frac{2\pi}{k\cos\theta} \left(\frac{1}{L_1 + L_{2A}} - \frac{1}{L_1 + L_{2B}}\right)^{-1}\ . \tag{54}$$

According to the geometry of figure 9, $R = L_{2B} - L_{2A}$. With the definition (10) for the Green's function this gives, after taking the $r^2 n\,|S(\omega)|^2$ terms into account,

$$T4 = \frac{n\,|S(\omega)|^2\,c}{2\cos\psi} \times r^2 \left(\frac{G(R)}{-i\omega}\right)^*\ . \tag{55}$$

Apart from the r^2-term and a complex conjugation of the Green's function, this term is similar to term 1 as given in expression (22). The r^2-term arises because both of the waves that are reflected upward from the reflector are proportional to the reflection coefficient. The fact that this contribution is multiplied with r^2 is simply due to the fact that both interfering waves that contribute to this term are proportional to r. The complex conjugate appears because the wave arrives at receiver A before it hits receiver B.

7 A NUMERICAL EXAMPLE

We present a numerical example of the theory. For simplicity we consider the theory in two dimensions. A reflector with reflection coefficient $r = 0.8$ is located at a depth 1500 m below the surface. This is not a small reflection coefficient, but since there is only one reflector and no free surface, this model does not generate any multiple reflections, regardless of how large the reflection coefficient is. The wave velocity is $c = 2000$ m/s, and the receivers are located at $\mathbf{r}_A = (0, 1000)$ m and $\mathbf{r}_B = (300, 500)$ m, respectively. We used noise sources at the surface with a spacing $\Delta x = 20$ m., and a Ricker wavelet with a dominant frequency of 50 Hz for the power spectrum $|S(\omega)|^2$ of the noise.

The contributions of the sources at the surface to the terms T1-T4 is shown in the left panel of figure 10, while the sum over all source positions is shown in the right panel. The right panel panels shows four distinct arrivals. The arrivals T1 and T3 are causal, while the arrivals T2 and T4 are acausal. T1 is the strongest arrival, because it does not depend on the reflection coefficient. The arrivals T2 and T3 are weaker, because they are the singly reflected waves, while the arrival T4 is the weakest because it varies as r^2.

Note that each of the arrivals in the right panel of figure 10 corresponds to a stationary source point in the left panel of that figure. The nonzero contribution of these arrivals is solely due to the stationary source points, the sources placed at other locations give contributions that interfere desctructively.

Figure 11 shows for term T3 a comparison between the exact waveform, computed with the 2D Green's function, that is shown with the solid line, and the term 3 obtained by summing the correlation over the sources at the surface (shown with crosses). The waveform obtained from seismic interferometry matches the exact waveform well. Note that the shown waveforms do not look like a Ricker wavelet; as theory predicts they are shifted over a phase angle equal to $\pi/4$.

The left panel of figure 10 shows weak arrivals between T1 and T4. These weak arrivals are due to endpoint contributions from the sum over the traces on the left panel of that figure, especially for the endpoints where the arrival time tends to a constant. In the numerical example we tapered the contribution of traces near the endpoints of the source region. Without this tapering these endpoint contributions are much stronger. This is of importance for virtual source imaging [Bakulin and Calvert, 2004] because a careless summation over all source positions may lead to endpoint contributions that could be confused with waves reflected off reflectors in the subsurface.

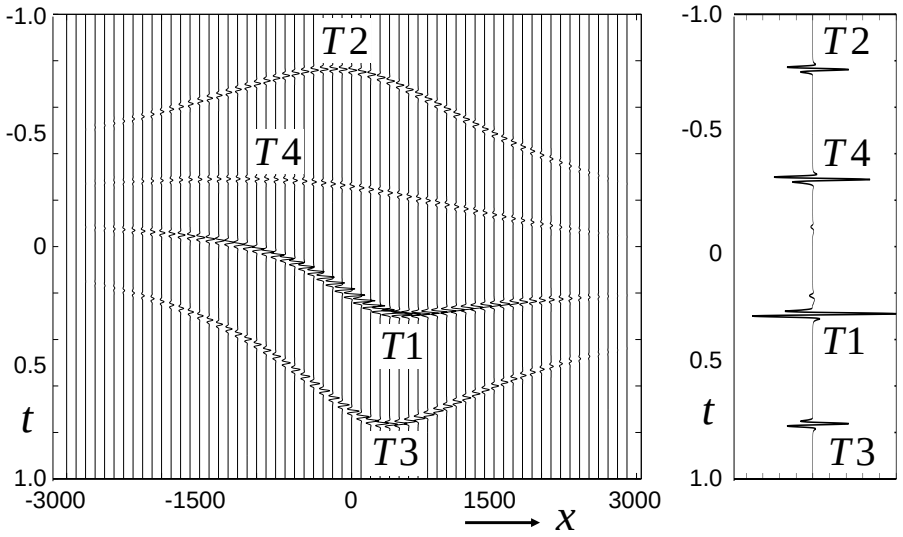

Figure 10. Left panel, the contribution of sources at the surface to the terms T1-T4 as a function of the source position x. For clarity only every fifth source position is shown. Right panel, the sum over all source positions at the surface.

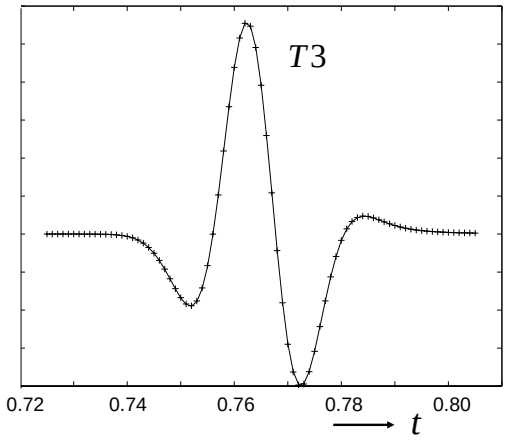

Figure 11. Solid line, the exact arrival for term T3 computed with the 2D Green's function. The crosses indicate the sum of the correlation for term T3 over all sources at the surface. This sum is tapered near the end of the source region.

8 THE CASE OF MORE THAN ONE REFLECTOR

Up to this point the analysis has been based on the assumption of a single reflector in the subsurface. Suppose there are more reflectors at depths D_j with reflection coefficients r_j. Assuming that the wave velocity remains constant, the second term in each of equations (11) needs to be replaced by a sum over all reflectors. In expression (12), the term T1 contains the direct waves only; this term is not influenced by the presence of more than one reflector. The terms T2 and T3 in expression (12) involve the cross term between the direct wave and the single-reflected waves. Since these terms are linear in the reflection coefficients, one can retrieve the sum of all the single reflected waves by summing the terms T2 and T3 over the different reflectors. This means that in the presence of more than one reflector, the cross terms T2 and T3 between the direct wave and the single-reflected waves produce the full set of single reflections.

The term T4 in expression (12) contains the product of the single reflected waves. This means that for more than one reflector this term contains double sum $\sum_{j,j'} r_j r_{j'}(\cdots)$. This double sum can be split into the terms $j' = j$ and the terms $j \neq j'$:

$$\sum_{j,j'} r_j r_{j'}(\cdots) = \sum_j r_j^2(\cdots) + \sum_{j \neq j'} r_j r_{j'}(\cdots) \qquad (56)$$

Analysis of the first term is identical to that of the term T4 in section **??**. This means that one can simply sum expression (55) over all reflectors in the subsurface.

The last contribution that needs to be accounted for is the contribution of the second sum in the right hand side of equation (56) to the term T4. We consider two reflectors at depths D_1 and D_2 with reflection coefficients r_1 and r_2, respectively. The derivation holds for any pair of reflectors. The wave paths associated with two different reflectors to term T4 is shown in figure 12. The integrand in the term T4 of expression (12) now contains a phase term $\exp ikL$ with

$$L = L_1^{(A)} + L_2^{(A)} - L_1^{(B)} - L_2^{(B)} \ , \qquad (57)$$

where these lengths are defined in figure 12. As before, the phase is stationary with respect to the y-coordinate

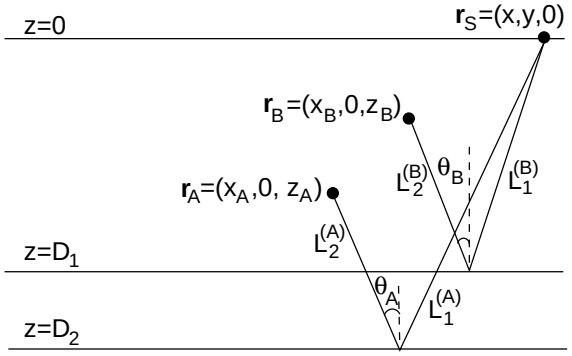

Figure 12. Definition of the geometric variables for the contribution of term 4 from waves reflected off two different reflectors.

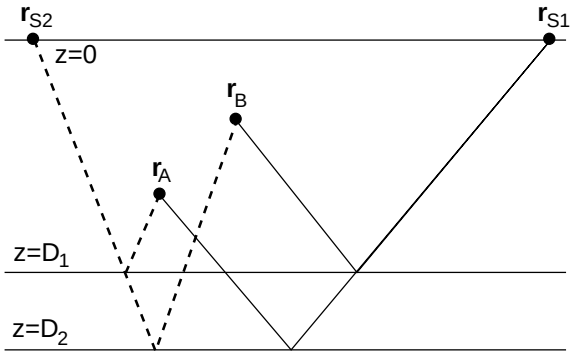

Figure 13. The stationary source points $\mathbf{r}_{S1}$ and $\mathbf{r}_{S2}$ for the correlation of waves reflected from two different reflectors. The corresponding wave paths to the receivers are shown with solid and dashed lines, respectively.

when $y = 0$. The condition that the phase is stationary with respect to x gives the condition

$$0 = \frac{\partial L}{\partial x} = \sin\theta_A - \sin\theta_B \ , \qquad (58)$$

where the angles θ_A and θ_B are defined in figure 12. This follows from the derivation that led to the first term in the right hand side of expression (35). The stationary phase condition for this term therefore gives

$$\theta_A = \theta_B \qquad , \qquad y = 0 \ . \qquad (59)$$

The stationary phase condition (59) gives two stationary source points $\mathbf{r}_{S1}$ and $\mathbf{r}_{S2}$ at the surface that are shown in figure 13. The wave paths shown in solid lines indicates the cross correlation of the waves that propagate along the following trajectories: $\mathbf{r}_{S1} \rightarrow$ reflector 1 $\rightarrow \mathbf{r}_B$ and $\mathbf{r}_{S1} \rightarrow$ reflector 2$\rightarrow \mathbf{r}_A$, while the wave paths shown in dashed lines indicate the correlation of the waves that propagate along the following trajectories: $\mathbf{r}_{S2} \rightarrow$ reflector 1 $\rightarrow \mathbf{r}_A$ and $\mathbf{r}_{S2} \rightarrow$ reflector 2 $\rightarrow \mathbf{r}_B$. These wave paths act as the direct and exchange scattering events in quantum mechanics [Lévy-Leblond and Balibur, 1990].

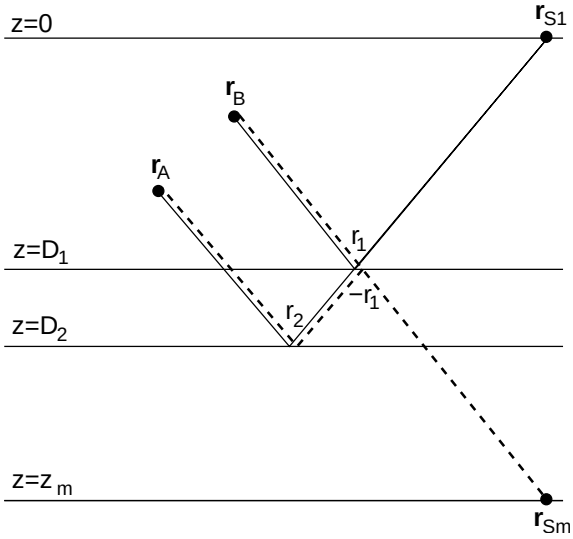

Figure 14. The stationary source points $\mathbf{r}_{S1}$ at the surface $z = 0$ and $\mathbf{r}_{Sm}$ at the surface $z = z_m$ for the correlation of waves reflected from two different reflectors. The corresponding wave paths to the receivers are shown with solid and dashed lines, respectively. The reflection coefficients for the different reflected waves are indicated.

The difference in the travel time of the waves that propagate along the two trajectories shown in the solid lines is not equal to the time it takes to propagate between the receivers. The stationary phase contributions that correspond to these cross terms are nonzero. This implies that the correlation of the waves reflected off different reflectors give stationary phase contributions that are proportional to $r_1 r_2$. These contributions depend on the product of reflection coefficients, hence the correlation of the single-reflected waves from different reflectors gives spurious arrivals that dynamically are equivalent to peg-leg multiples that are reflected once from the free surface and twice from reflectors in the subsurface, because the peg-leg surface multiples are also proportional to $r_1 r_2$.

This is a puzzling conclusion, since theory predicts that the full Green's function can be retrieved when the sources are placed on a closed surface that surrounds the region of interest [Wapenaar et al., 2004; Wapenaar et al., 2005]. The key point is that in the derivation of this paper the sources are placed at the upper surface only. Let us consider what would happen if we also had sources at a surface $z = z_m$ that is located below the reflectors as shown in figure 14.

The reflection response and transmission response of the subsurface are not independent [Claerbout, 1968; Wapenaar et al., 2004]. This suggests that sources below the reflectors are essential for the cancellation of the cross-terms on singly-reflected waves, and we provide a heuristic argument that this is indeed the case.

Consider the situation in figure 14 where sources

are present at the surface $z = 0$ above the reflectors, and at the surface $z = z_m$ below the reflectors. The points $\mathbf{r}_{S1}$ and $\mathbf{r}_{Sm}$ on these surfaces are the stationary source points for the cross-terms that correspond to the path indicated with solid lines and dashed lines, respectively. The waves excited at the surface $z = 0$ propagate along the paths shown with solid lines, while the waves excited below the reflectors propagate along the paths shown in dashed lines. These wave paths coincide after their first encounter with reflector 1, hence the contribution of waves radiated from the stationary point; $\mathbf{r}_{S1}$ and $\mathbf{r}_{Sm}$ to the cross-correlation is nonzero for the same delay time. The contribution of the waves excited at $\mathbf{r}_{S1}$ is proportional to $r_1 r_2$, while the contribution of the waves excited at $\mathbf{r}_{Sm}$ is equal to $-r_1 r_2$, because the reflection coefficient of reflector 1 for a downward reflected waves is $-r_1$ rather than r_1. As shown in the examples in the previous sections, it does not matter how far the stationary point is removed from the surface. Therefore, the stationary points $\mathbf{r}_{S1}$ and $\mathbf{r}_{Sm}$ give contributions to the cross-correlation that are equal, but have opposite sign. This means that the sum of the cross terms of the cross-correlation of these two stationary points gives a vanishing contribution.

In practical situations the sources are typically located at the surface $z = 0$ only; this is for example the case in the virtual-source experiment of Bakulin and Calvert [2004]. In that case the cross terms of waves reflected from different reflectors give a non-zero contribution that is proportional to the product of reflection coefficients. These non-zero contributions are proportional to the product of reflection coefficients. Therefore, virtual source imaging introduces spurious multiples when the sources cannot be placed on a closed surface.

9 DISCUSSION

Inserting expression (22), (47), (48) and (55) into equation (12) gives for one reflector the following total contribution to the correlation:

$$C_{AB}(\omega) = \frac{n\,|S(\omega)|^2\,c}{2\cos\psi}\left\{\frac{G(R)}{-i\omega} + r^2\left(\frac{G(R)}{-i\omega}\right)^* + r\,\frac{G(R_1+R_2)}{-i\omega} + r\left(\frac{G(R_1+R_2)}{-i\omega}\right)^*\right\}. \tag{60}$$

In the presence of more reflectors, one can sum the last three terms over the different reflectors. The correlation is a weighted average of the causal and acausal Green's function for the direct wave and the singly-reflected waves. Note that for the direct wave, the acausal Green's function is weighted by r^2. This is because the contribution of upgoing waves is r^2 times the contribution to the Green's function from the downgoing waves. In practical applications of seismic interferometry in reflection seismology, this contribution to the direct waves is not relevant because the primary reflections rather than the direct waves are used to image the subsurface.

Note that it is arbitrary how the cross-correlation is defined. When the cross-correlation is defined by $C_{AB}(\omega) = u_A^*(\omega)u_B(\omega)$ instead of expression (6) the roles of the causal and acausal Green's functions are interchanged. Since in practice one extracts the causal Green's function from the correlation, this arbitrariness in the definition of the correlation does not matter.

The four terms in expression (60) correspond to the waves that propagate along the four trajectories shown in figure 15. The waves in the upper diagrams are the direct waves that propagate in opposite directions between the two receivers. The waves in the bottom diagrams are the single-reflected waves that propagate in opposite directions between the receivers. These diagrams provide an illustration of why the correlation leads to the superposition of the causal and acausal Green's function.

In the derivation of this paper we did not explicitly account for the radiation pattern of the point source. It follows from the figure 15 (and figure A1 for a heterogeneous medium) that the paths that render the phase of the correlation stationary correspond to rays that propagate in the same direction to the two receivers. This means that if the source does not radiate energy isotropically, the two receivers are still illuminated with the same source strength. Similarly, when the reflection coefficient depends on the angle of incidence, the stationary phase approximation selects the reflection angle at the angle of the reflected wave that propagates between the receivers A and B, as shown in figure 15.

When more reflectors are present, the contribution of term 4 is proportional to $r_j r_{j'}$. When only sources at the surface $z = 0$ are used, these cross terms lead to spurious multiples that have the same strength as peg-leg multiples. These spurious multiples are not removed by algorithms for the removal of surface-related multiples [Verschuur et al, 1992; van Borselen et al., 1996; Dragoset and Jeričević, 1998] because kinematically they do not correspond to peg-leg multiples.

The analysis of this paper shows that the Green's function is retrieved from the stationary phase contribution from the integration (summation) over all sources. The sources far from the stationary point give an oscillatory contribution that averages to zero. When random noise is used as a source, these source in general are spread out over the surface. When man-made sources are used, however, one may limit these sources to the stationary phase region.

Acknowledgments: We appreciate the comments of John Stockwell, and Kurang Mehta.

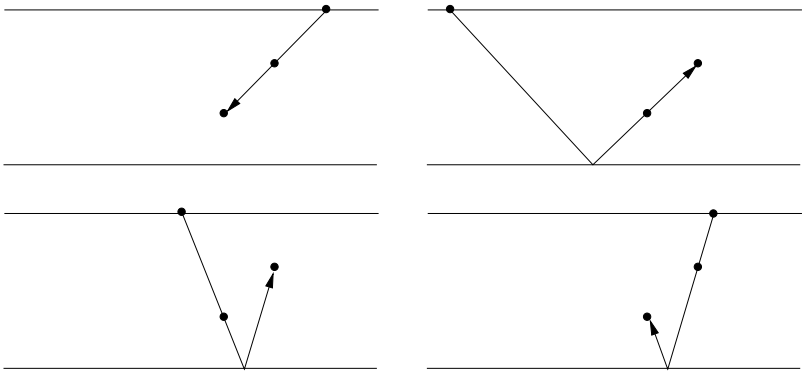

Figure 15. The wave paths that correspond to the stationary contributions to the correlations for the causal direct wave from term 1 (upper left panel), the acausal direct wave from term 4 (upper right panel), the acausal reflected wave from term 2 (lower left panel), the causal reflected wave from term 3 (lower left panel).

REFERENCES

A. Bakulin and R. Calvert. Virtual source: new method for imaging and 4D below complex overburden. *Expanded abstracts of the 2004 SEG-meeting*, pages 2477–2480, 2004.

M. Berrry and C. Upstill. Catastrophe optics: Morphologies of caustics and their diffraction patterns. In E. Wolf, editor, *Prog. in Optics, XVIII*, pages 257–346. 1980.

N. Bleistein. *Mathematical Methods for Wave Phenomena*. Academic Press, Orlando, 1984.

N. Bleistein, J.K. Cohen, and J.W. Stockwell Jr. *Mathematics of Multidimensional Seismic Imaging, Migration, and Inversion*. Springer, New York, 2001.

O.M. Bucci and G Franceschetti. On the degrees of freedom of scattered fields. *IEEE Trans. on Antennas and Propagation*, 37:918–926, 1989.

M. Campillo and A. Paul. Long-range correlations in the diffuse seismic coda. *Science*, 299:547–549, 2003.

V. Cervený and F. Hron. The ray series method and dynamical ray tracing system for three-dimensional inhomogeneous media. *Bull. Seismol. Soc. Am.*, 70:47–77, 1980.

J.F. Claerbout. Synthesis of a layered medium from its acoustic transmission response. *Geophysics*, 33:264–269, 1968.

A. Derode, E. Larose, M. Campillo, and M. Fink. How to estimate the Green's function for a heterogeneous medium between two passive sensors? Application to acoustic waves. *Appl. Phys. Lett.*, 83:3054–3056, 2003a.

A. Derode, E. Larose, M. Tanter, J. de Rosny, A. Tourin, M. Campillo, and M. Fink. Recovering the Green's function from far-field correlations in an open scattering medium. *J. Acoust. Soc. Am.*, 113:2973–2976, 2003b.

W.H. Dragoset and Z. Jeričević. Some remarks on multiple attenuation. *Geophysics*, 63:772–789, 1998.

M. Haney and R. Snieder. Seismic data processing in the stationary phase approximation. *First Break, in press*, 2005.

H.J. Landau. Necessary density conditions for sampling and interpolation of certain entire functions. *Acta Mathematica*, 117:37–52, 1967.

E. Larose, A. Derode, M. Campillo, and M. Fink. Imaging from one-bit correlations of wideband diffuse wave fields. *J. Appl. Phys.*, 95:8393–8399, 2004.

Lévy-Leblond and F. Balibur. *Quantics, Rudiments of Quantum Physics*. North-Holland, Amsterdam, 1990.

O.I. Lobkis and R.L. Weaver. On the emergence of the Green's function in the correlations of a diffuse field. *J. Acoust. Soc. Am.*, 110:3011–3017, 2001.

A. Malcolm, J. Scales, and B.A. van Tiggelen. Extracting the Green's function from diffuse, equipartitioned waves. *Phys. Rev. E*, 70:015601, 2004.

J.E. Rickett and J.F. Claerbout. Acoustic daylight imaging via spectral factorization; helioseismology and reservoir monitoring. *The Leading Edge*, 18:957–960, 1999.

J.E. Rickett and J.F. Claerbout. Calculation of the sun's acoustic impulse response by multidimensional spectral factorization. *Solar Physics*, 192:203–210, 2000.

P. Roux and M. Fink. Green's function estimation using secondary sources in a shallow water environment. *J. Acoust. Soc. Am.*, 113:1406–1416, 2003.

P. Roux, K.G. Sabra, W.A. Kuperman, and A. Roux. Ambioent noise cross correlation in free space: Theoretical approach. *J. Acoust. Soc. Am.*, 117:79–84, 2005.

K.G. Sabra, P. Roux, and W.A. Kuperman. Arrival-time structure of the time-averaged ambient noise cross-correlation in an oceanic waveguide. *J. Acoust. Soc. Am.*, 117:164–174, 2005.

G.T. Schuster, J. Yu, J. Sheng, and J. Rickett. Interferometric/daylight seismic imaging. *Geophys. J. Int.*, 157:838–852, 2004.

N.M. Shapiro and M. Campillo. Emergence of broadband Rayleigh waves from correlations of the ambient seismic noise. *Geophys. Res. Lett.*, 31:L07614, doi10.1029/2004GL019491, 2004.

N.M. Shapiro, M. Campillo, L. Stehly, and M.H. Ritzwoller. High-resolution surface-wave tomography from ambient seismic noise. *Science*, 307:1615–1618, 2005.

R. Snieder. Extracting the Green's function from the correlation of coda waves: A derivation based on stationary phase. *Phys. Rev. E*, 69:046610, 2004a.

R. Snieder. *A Guided Tour of Mathematical Methods for the Physical Sciences*. Cambridge Univ. Press, Cambridge, UK, 2nd edition, 2004b.

R. Snieder. Extracting the building response from an incoherent excitation; theory and application to the Millikan Library in Pasadena, California. *Project Review of the Consortium Project on Seismic Inverse Methods for*

Complex Structures, 2005.

R. Snieder and C. Chapman. The reciprocity properties of geometrical spreading. *Geophys. J. Int.*, 132:89–95, 1998.

R. Snieder and A. Lomax. Wavefield smoothing and the effect of rough velocity perturbations on arrival times and amplitudes. *Geophys. J. Int.*, 125:796–812, 1996.

R.G. van Borselen, J.T. Fokkema, and P.M. van den Berg. Removal of surface-related wave phenomena - the marine case. *Geophysics*, 61:202–210, 1996.

D.J. Verschuur, A.J. Berkhout, and C.P.A. Wapenaar. Adaptive surface-related multiple elimination. *Geophysics*, 57:1166–1177, 1992.

K. Wapenaar. Retrieving the elastodynamic Green's function of an arbitrary inhomogeneous medium by cross correlation. *Phys. Rev. Lett.*, 93:254301, 2004.

K. Wapenaar, J. Fokkema, and R. Snieder. Retrieving the Green's function by cross-correlation: a comparison of approaches. *Submitted to J. Acoust. Soc. Am.*, 2005.

K. Wapenaar, J. Thorbecke, and D. Dragonov. Relations between reflection and transmission responses of three-dimensional inhomogeneous media. *Geophys. J. Int.*, 156:179–194, 2004.

R.L. Weaver and O.I. Lobkis. Ultrasonics without a source: Thermal fluctuation correlations and MHz frequencies. *Phys. Rev. Lett.*, 87:134301–1/4, 2001.

R.L. Weaver and O.I. Lobkis. Diffuse fields in open systems and the emergence of the green's function. *J. Acoust. Soc. Am.*, 116:2731–2734, 2004.

O. Yilmaz. Seismic data processing. In *Investigations in geophysics*, volume 2. Society of Exploration Geophysicists, Tulsa, 1987.

APPENDIX A: SEISMIC INTERFEROMETRY OF THE DIRECT WAVES IN THE RAY-GEOMETRIC APPROXIMATION

In this appendix, we show that the arguments used in this paper for a homogeneous medium can be generalized to heterogenous media where the velocity variations are sufficiently smooth to justify the use of ray theory for the Green's function. In order to avoid complications due to curved reflectors, we analyze only term T1. For simplicity we assume that the density is constant. The ray-geometric Green's function that gives the response at $\mathbf{r}_1$ due to a point source in $\mathbf{r}_2$ is given by expression (15) of [Snieder and Chapman, 1998]:

$$G^{ray}(\mathbf{r}_1,\mathbf{r}_2) = -\frac{1}{4\pi}\sqrt{\frac{v_1}{v_2}}\frac{\exp\left(i\omega\tau_{12}\right)}{\sqrt{J_{12}}}\,. \qquad \text{(A1)}$$

In this expression $v_1 = v(\mathbf{r}_1)$, τ_{12} is the travel time for the propagation from $\mathbf{r}_2$ to $\mathbf{r}_1$, and J_{12} is the associated geometrical-spreading factor. Because of reciprocity [Snieder and Chapman, 1998], this Green's function is also equal to

$$G^{ray}(\mathbf{r}_1,\mathbf{r}_2) = -\frac{1}{4\pi}\sqrt{\frac{v_2}{v_1}}\frac{\exp\left(i\omega\tau_{21}\right)}{\sqrt{J_{21}}}\,. \qquad \text{(A2)}$$

Note that the travel time is reciprocal:

$$\tau_{12} = \tau_{21}\,, \qquad \text{(A3)}$$

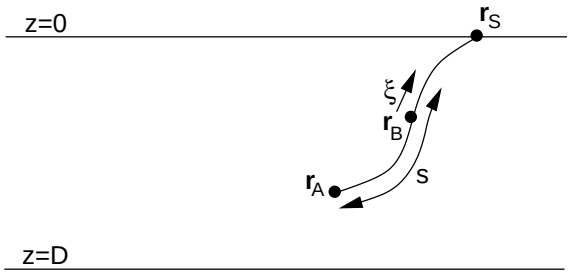

Figure A1. The stationary phase condition for term 1 for a heterogeneous reference medium.

but the geometrical spreading is not [Snieder and Chapman, 1998].

Inserting the Green's function (A2) in term T1 of expression (12) gives

$$T1 = \frac{1}{(4\pi)^2}\int \frac{v_S}{\sqrt{v_A v_B}}\frac{\exp\left(i\omega\left(\tau_{SA}-\tau_{SB}\right)\right)}{\sqrt{J_{SA}J_{SB}}}dxdy\,, \qquad \text{(A4)}$$

where $v_S = v(\mathbf{r}_S) = v(x,y,0)$, $v_A = v(\mathbf{r}_A)$, and $v_B = v(\mathbf{r}_B)$. By analogy with the situation shown in figure 3 the stationary points in this integral correspond to the rays that propagate from the source S through receiver B to receiver A as shown in figure A1. By virtue of reciprocity, these stationary points can be found by tracing rays from receiver A to receiver B and by continuing these rays to the surface $z = 0$. In general there may be more than one stationary point. In the following we analyze the contribution of one stationary point, but in the end one needs to sum over all stationary points. It may happen, in fact, that the region of stationary phase does not consist of a finite number of points, but of a line or surface area. In that case, point A is a caustic and ray theory breaks down [Berry and Upstill, 1980].

Let the travel time along the ray from A to B to S be given by τ_0. The travel time for an adjacent ray follows from the second-order Taylor expansion in the ray-centered coordinates q_1 and q_2 that measure the perpendicular distance to the ray in two orthogonal directions. According to expression (50) of Cervený and Hron [1980] the travel time along an adjacent ray is given by

$$\tau = \tau_0 + \frac{1}{2}\mathbf{q}\cdot\mathbf{M}\cdot\mathbf{q}\,, \qquad \text{(A5)}$$

with $\mathbf{M}$ a matrix of second-order derivatives of the travel time. In the following it is convenient to replace the integration over the surface $z = 0$ in expression (A4) by an integration over the ray-centered coordinates q_1 and q_2. The orientation of these coordinate axes is ambiguous, since any choice of axes perpendicular to the ray is admissible. In the following we choose the q_2-axis to be aligned with the plane $z = 0$, as indicated in figure A2. The other coordinate, q_1, then measures the distance to the ray in the orthogonal direction. As shown in figure A2, the associated q_1-axis makes an angle ψ with the horizontal that is equal to the angle between

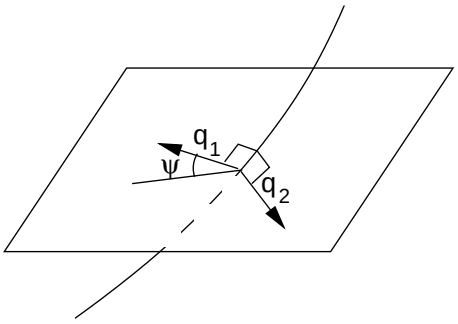

Figure A2. Definition of the ray-centered coordinates q_1 and q_2. The q_2-axis lies in the x, y-plane and is perpendicular to the ray. The angle ψ is the angle between the ray direction and the vertical.

the ray and the vertical. An element dq_2 corresponds to an element dy' in the x, y-plane, while an element dq_1 corresponds to an element $dq_1 = \cos\psi dx'$. We use primed coordinates since the ray direction is not necessarily aligned with the original x-axis. This means that a surface element in the surface integral can be related to a surface element $dq_1 dq_2$ using

$$dxdy = dx'dy' = \frac{1}{\cos\psi} dq_1 dq_2 \ . \tag{A6}$$

This expression can be used to evaluate integral (A4) in the stationary phase approximation. With Taylor expansion (A5) for the rays from A to S and from B to S, this integral in the stationary phase approximation is given by

$$T1 = \frac{1}{(4\pi)^2 \cos\psi} \frac{v_S}{\sqrt{v_A v_B}} \frac{\exp\left(i\omega\left(\tau_{SA} - \tau_{SB}\right)\right)}{\sqrt{J_{SA} J_{SB}}} \times \int \exp\left(\frac{i\omega}{2} \mathbf{q} \cdot \left(\mathbf{M}_{SA} - \mathbf{M}_{SB}\right) \cdot \mathbf{q}\right) dq_1 dq_2 \ . \tag{A7}$$

The integration over the q-variables gives [Bleistein, 1984]

$$T1 = \frac{1}{8\pi\omega \cos\psi} \frac{v_S}{\sqrt{v_A v_B}} \frac{\exp\left(i\omega\left(\tau_{SA} - \tau_{SB}\right)\right)}{\sqrt{J_{SA} J_{SB}}} \frac{\exp\left(isgn\ \pi/4\right)}{\sqrt{\left|\det\left(\mathbf{M}_{SA} - \mathbf{M}_{SB}\right)\right|}} \ , \tag{A8}$$

where sgn is the number of positive eigenvalues of $\mathbf{M}_{SA} - \mathbf{M}_{SB}$ minus the number of negative eigenvalues. Using the same reasoning as in the derivation of expression (6.21) of [Snieder and Lomax, 1996], $T1$ is equal to

$$T1 = \frac{i}{8\pi\omega \cos\psi} \frac{v_S}{\sqrt{v_A v_B}} \frac{\exp\left(i\omega\left(\tau_{SA} - \tau_{SB}\right)\right)}{\sqrt{J_{SA} J_{SB} \det\left(\mathbf{M}_{SA} - \mathbf{M}_{SB}\right)}} \ . \tag{A9}$$

Since the points $\mathbf{r}_A$, $\mathbf{r}_B$, and $\mathbf{r}_S$ are located on the same ray,

$$\tau_{SA} - \tau_{SB} = \tau_{AB} \ , \tag{A10}$$

this is the travel time along the ray that joins the receivers A and B. This means that $T1$ is kinematically identical to the Green's function that accounts for the wave propagation between the receivers A and B. In the following we show that expression (A9) also accounts dynamically for this Green's function by using a derivation similar to that presented in [Snieder and Lomax, 1996].

According to expression (68) of Cervený and Hron [1980], the matrix $\mathbf{M}$ is related to the curvature matrix of the wavefronts by the relation

$$\mathbf{M} = \frac{1}{v} \mathbf{K} \ . \tag{A11}$$

Since $\mathbf{M}$ is a 2×2 matrix this, together with expression (A10), implies that

$$T1 = \frac{i}{8\pi\omega \cos\psi} \frac{v_S^2}{\sqrt{v_A v_B}} \frac{\exp\left(i\omega\tau_{AB}\right)}{\sqrt{J_{SA} J_{SB} \det\left(\mathbf{K}_{SA} - \mathbf{K}_{SB}\right)}} \ . \tag{A12}$$

Following equation (76) of Cervený and Hron [1980], the curvature matrix satisfies the following matrix Ricatti equation:

$$\frac{d\mathbf{K}_{SA}}{ds} = \frac{1}{v} \frac{dv}{ds} \mathbf{K}_{SA} - \mathbf{K}_{SA}^2 - \frac{1}{v} \mathbf{V} \ , \tag{A13}$$

where $v = v_S$, and the matrix $\mathbf{V}$ is defined by $V_{ij} = \partial^2 v / \partial q_i \partial q_j$, and where s is the distance along the ray from $\mathbf{r}_A$ through $\mathbf{r}_B$ to the surface, as indicated in figure A1. Using this expression, and the corresponding expression for $\mathbf{K}_{SB}$ it follows that the difference satisfies the following differential equation

$$\frac{d\left(\mathbf{K}_{SA} - \mathbf{K}_{SB}\right)}{ds} = \frac{1}{v} \frac{dv}{ds} \left(\mathbf{K}_{SA} - \mathbf{K}_{SB}\right) - \left(\mathbf{K}_{SA}^2 - \mathbf{K}_{SB}^2\right) \ . \tag{A14}$$

From this it follows after a lengthy calculation that

$$\frac{d}{ds} \det\left(\mathbf{K}_{SA} - \mathbf{K}_{SB}\right) = \frac{2}{v} \frac{dv}{ds} \det\left(\mathbf{K}_{SA} - \mathbf{K}_{SB}\right) - \left(tr\ \mathbf{K}_{SA} + tr\ \mathbf{K}_{SB}\right) \det\left(\mathbf{K}_{SA} - \mathbf{K}_{SB}\right) \ , \tag{A15}$$

where tr denotes the trace. According to expression (70) of Snieder and Chapman [1998]

$$tr\ \mathbf{K} = \frac{1}{J} \frac{dJ}{ds} \ . \tag{A16}$$

Using this expression to eliminate the trace of $\mathbf{K}_{SA}$ and $\mathbf{K}_{SB}$ from expression (A15), the result can be integrated to give

$$\frac{d}{ds} \left\{ \frac{J_{SA} J_{SB} \det\left(\mathbf{K}_{SA} - \mathbf{K}_{SB}\right)}{v_S^2} \right\} = 0 \ , \tag{A17}$$

or

$$\frac{J_{SA} J_{SB} \det\left(\mathbf{K}_{SA} - \mathbf{K}_{SB}\right)}{v_S^2} = const. \tag{A18}$$

This expression holds for any point S along the ray in figure A1. The constant can be found by evaluating this expression for a point S along the ray at a small distance ξ beyond the receiver B, as shown in figure A1, and by letting this distance go to zero. At a small distance from receiver B, the medium can be considered to be locally homogeneous, and the curvature matrix attains its value for a homogeneous medium:

$$\mathbf{K}_{SB} = \begin{vmatrix} 1/\xi & 0 \\ 0 & 1/\xi \end{vmatrix} . \qquad \text{(A19)}$$

In the limit $\xi \rightarrow 0$ these terms dominate the contributions from $\mathbf{K}_{SA}$ in expression (A18) and $\det(\mathbf{K}_{SA} - \mathbf{K}_{SB}) \rightarrow 1/\xi^2$ as $\xi \rightarrow 0$. In that limit the geometrical spreading is given by $J_{SB} = \xi^2$, $J_{SA} \rightarrow J_{BA}$, and $v_S \rightarrow v_B$. Inserting these results in expression (A12) shows that the constant in that expression is given by $const = J_{BA}/v_B^2$. Inserting this in expression (A18) finally gives

$$J_{SA} J_{SB} \det(\mathbf{K}_{SA} - \mathbf{K}_{SB}) = \frac{v_S^2}{v_B^2} J_{BA} , \qquad \text{(A20)}$$

or

$$\sqrt{J_{SA} J_{SB} \det(\mathbf{K}_{SA} - \mathbf{K}_{SB})} = \pm \frac{v_S}{v_B} \sqrt{J_{BA}} . \qquad \text{(A21)}$$

At this point, the sign in the right hand side is arbitrary.

This last result can be used to eliminate $\sqrt{\det(\mathbf{K}_{SA} - \mathbf{K}_{SB})}$ from expression (A12), giving

$$T1 = \frac{\pm i v_S}{8\pi\omega \cos\psi} \sqrt{\frac{v_B}{v_A}} \frac{\exp(i\omega\tau_{AB})}{\sqrt{J_{BA}}} . \qquad \text{(A22)}$$

Following expression (45) of Snieder and Chapman [1998], the reciprocity property of the geometrical spreading is given by $J_{BA} = (v_B/v_A)^2 J_{AB}$; hence

$$T1 = \frac{\pm i v_S}{8\pi\omega \cos\psi} \sqrt{\frac{v_A}{v_B}} \frac{\exp(i\omega\tau_{AB})}{\sqrt{J_{AB}}} . \qquad \text{(A23)}$$

A comparison with the ray-geometric Green's function (A1) gives

$$T1 = \frac{\mp v_S}{2\cos\psi} \times \frac{G^{ray}(\mathbf{r}_A, \mathbf{r}_B)}{-i\omega} . \qquad \text{(A24)}$$

After multiplying with the terms $n\,|S(\omega)|^2$, this result can directly be compared with the corresponding expression (22) for a homogeneous medium. This implies that the lower sign in expression (A21) must be used. After taking the source spectrum and the scatterer density into account, this finally gives equation (24).